Published in final edited form as:

Magn Reson Imaging. 2018 April ; 47: 97–102. doi:10.1016/j.mri.2017.11.003.

White Matter Structural Integrity and Trans-Cranial Doppler Blood Flow Pulsatility in Normal Aging

Roman Fleysher[a,b,*], **Michael L Lipton**[a,b,c,d], **Olga Noskin**[g], **Tatjana Rundek**[h], **Richard Lipton**[e,f], and **Carol A. Derby**[e,f]

[a]The Gruss Magnetic Resonance Research Center, Bronx, NY, United States

[b]Department of Radiology, Bronx, NY, United States

[c]Department of Psychiatry and Behavioral Sciences, Bronx, NY, United States

[d]The Dominick P. Purpura Department of Neuroscience, Bronx, NY, United States

[e]Saul R Korey Department of Neurology, Bronx, NY, United States

[f]Department of Epidemiology and Population Health, Albert Einstein College of Medicine and Montefiore Medical Center, Bronx, NY, United States

[g]Neurology Group of Bergen County, P. A., Ridgewood, NJ, United States

[h]Departments of Neurology and Public Health Sciences, University of Miami Miller School of Medicine, Miami, FL, United States

Abstract

Cerebrovascular diseases underlie many forms of age-related cognitive impairment and the mechanism linking the two is hypothesized to involve adverse changes in white matter (WM) integrity. Despite being systemic, small vessel disease does not uniformly affect WM. We performed voxel-wise analysis of MRI images to examine the association between fractional anisotropy (FA) — a diffusion tensor measure of WM structural integrity — and pulsatility index (PI) — a transcranial Doppler ultrasound measure of abnormal arterial flow — in adults over the age of 70 years who were free of stroke and dementia. We demonstrate that the relation of PI to microstructural changes in WM is artery specific and regional. We identified spatial clusters of significant correlations between elevated PI and reduced FA which can not be explained by aging, supporting a vascular hypothesis of WM injury. These areas are not limited to the vascular territories of the vessels where PI is assessed, suggesting that the linkage between PI and FA is not likely a function of perfusion per se, but is consistent with injury caused by mechanical wave emanating from pulsating vessel walls.

[*]Corresponding author: Roman.Fleysher@einstein.yu.edu.

Keywords

DTI; TCD; aging; white matter structural integrity; fractional anisotropy; pulsatility index

1. Introduction

Growing recognition that cerebrovascular diseases underlie many forms of age-related cognitive decline and dementia [1–5] makes vascular risk factors important targets for intervention. Whether vascular pathology exacerbates the impairment or whether the two are synergistic remains unclear, but the mechanism linking the two is believed to involve white matter (WM) injury. At advanced stages, this injury manifests as white matter hyperintense (WMHI) lesions on T2-weighted FLAIR MRI images [4, 6] and is reportedly associated with elevated blood flow pulsatility index (PI) — a marker of cerebrovascular small vessel disease — in normal elderly population [7–13]. Given that WMHIs result from a long term accumulated WM damage, linking PI to white matter pathology at an earlier stage, before onset of dementia, may provide a tool to screen and monitor population at risk for developing it later in life.

Two groups investigated the relationship between pulsatility index and fractional anisotropy (FA) — an early marker of WM integrity [14] as assessed by diffusion tensor imaging (DTI) — with conflicting results [12, 13]. Based on the premise that small vessel disease diffusely affects all intracranial arteries and the entire brain, these studies examined the association between pulsatility index and FA averaged over large predefined white matter regions. The first study found a strong association between elevated pulsatility and reduced average white matter FA [12], while the second observed no significant relation in similar brain areas in patients of similar group [13].

The discordance between results of these studies may be attributed to several factors: PI was measured using different techniques (MRI versus transcranial Doppler (TCD) ultrasound) and in different arteries (basilar and carotid versus middle cerebral arteries), DTI acquisitions used drastically different b-values (3000 versus 700 sec/mm^2). Because both studies operated under the same hypothesis that FA changes are not limited to the vascular territories of the arteries where pulsatility is evaluated, choice of arteries was driven by measurement convenience, PI from left and right arteries were averaged and FA was averaged over large regions. These factors may decrease sensitivity of the analyses or distort their results if, in fact, another hypothesis is true.

Pulsatility index refers to the Gossling pulsatility index (PI) expressed as the ratio of the range of the blood flow velocity over the cardiac cycle to its mean [15]. By this definition, PI in aorta is expected to differ from PI in carotid arteries and indeed anatomical differences in left and right vascularization may be sufficient to cause lateral differences in PI [16]. Therefore, we hypothesized that the predictive value of PI with respect to FA changes in white matter may be expected to depend on the artery in which it is being assessed. Moreover, although small vessel disease is systemic, its diffuse character does not imply that the brain is uniformly affected. The degree to which WM is susceptible to vascular disease and is damaged by it may vary with spatial location or limited to specific vascular territories.

Consequently, performing analysis without spatially averaging FAs and pulsatilities will increase sensitivity to detect such spatially heterogeneous processes.

In this study we apply a voxel-wise approach to examine relationship between white matter integrity assessed using FA and TCD-derived pulsatility index in the major cerebral arteries of normal elderly subjects. We determine in which cerebral artery PI has the strongest association with changes in FA. We then contemplate as to the possible causal mechanism of the observed relationships between PI and FA.

2. Materials and Methods

2.1. Subject Enrollment

This study was approved by the institutional review board of Albert Einstein College of Medicine. The analysis includes 107 participants in the Einstein Aging Study (EAS) cohort who gave written informed consent, were English-speaking, non-demented, over the age of 70 and who completed TCD and MRI evaluations at an annual study clinic visit between June 2012 and February 2015. EAS participants were recruited through systematic sampling from Medicare and voter registration lists for Bronx County, New York [17]. EAS participants receive annual in-person assessments which include medical history, neuropsychological testing and general medical and neurological examinations. Exclusion criteria included visual or auditory impairments that preclude neuropsychological testing, active psychiatric symptomatology that interfered with the ability to complete assessments, and non-ambulatory status. Dementia diagnosis was based on consensus case conference using standardized clinical criteria. Details of the EAS study design and methods are described previously [17].

2.2. TCD measurements

Complete, bilateral transcranial Doppler sonography in the supine position was performed by a certified technologist using a single gate, non-imaging Pioneer TC8080™ system (Viasys Healthcare Inc.) using a 2MHz transducer according to the guidelines of the American Institute of Ultrasound in Medicine [18]. TCD examination assessed blood flow velocities in the vertebral arteries (VA at a 60 mm depth) and basilar artery (BA a 90–100 mm depth) through a “transforaminal window”; and the middle cerebral arteries (MCA; distal M1 segment at a 50–65 mm depth), the posterior cerebral arteries (PCA; P1 segment at a 60–65 mm depth) and the anterior cerebral arteries (ACA; A1 at a 60–70 mm depth) through a temporal “acoustic window”. Blood flow velocity in these nine arteries was analyzed off-line using the imaging reading work station (ImagePro). Specifically, we measured: peak systolic velocity (PSV), end-diastolic velocity (EDV) and mean flow velocity (MFV). The pulsatility index was calculated using the Gosling equation, $PI = (PSV - EDV)/MFV$ [15]. Because PI is defined as the ratio of the velocities, it is not sensitive to the orientation of the probe with respect to the direction of the flow in the vessel. TCD measures could not be obtained in all vessels in all subjects due to normal variations of anatomy and availability of acoustic windows. To increase sensitivity of the analyses, we included all available data for each vessel.

2.3. MRI Image Acquisition and Preprocessing

The imaging was performed using a 3.0T Philips Achieva TX scanner (Philips Medical Systems, Best, The Netherlands) utilizing its 32-channel head coil and the following protocol: T1-weighted 3D MPRAGE with TR/TE/TI=9.9/4.6/900msec, flip angle 8°, $1mm^3$ isotropic resolution, 240×188×220 matrix; DTI using 2D single-shot EPI with 32 diffusion encoding directions, b-value=800sec/mm^2, TR=10sec, TE=65msec, $2mm^3$ isotropic resolution, 128×120 matrix, 70 slices; and an auxiliary 3D B_0 field map using a dual echo gradient echo technique with TR/TE/ΔTE=20/2.4/2.3ms; $4mm^3$ isotropic resolution, flip angle, 20° to correct EPI distortions in DTI and small distortions in T1-weighted images.

Data from all subjects was first preprocessed individually and then registered to a common template for group analysis. First, non-brain voxels were removed from all images using the FMRIB-FSL software [19, 20]. Subsequently, eddy current correction followed by tensor fitting of the diffusion data to produce maps of fractional anisotropy (FA) and image unweighted for diffusion (the S0 image) were performed using FSL's diffusion toolbox [21]. Then, EPI distortion in S0 and FA maps was removed using FUGUE of FSL utilizing auxiliary field map [22]. To achieve the best registration of the field map to DTI, field map was first distorted the same way the DTI is distorted and then the rigid body transformation needed to match it to the DTI was appled to the original field map. Although this field map does not match the DTI image when overlaid — one is still distorted the other is not — it is actually properly registered and ready to be used in FUGUE [23]. Small distortions in the T1-weighted image caused by magnetic field inhomogeneities around sinuses were removed in the same fashion. Finally, rigid body transformation was applied to FA map to register it to the T1-weighted image. Similar to the use of gray and white matter masks to increase robustness of registration of images to a template [24], all rigid body transformations were obtained as ones needed to register white matter masks segmented out by the FAST routine of FSL from the input and target images.

2.4. Registration to a Study-Specific Template

Following the intra-subject preprocessing, FA map from each subject was registered to a common T1-weighted image template using nonlinear registration module of ART [25–27]. Because quality of registration to a template is sensitive to the similarity of a brain to the template, to improve the overall quality we selected a study-specific "central" template — a template requiring least average deformation of the brains in the study — with the idea that smaller deformations are accompanied by smaller registration errors [28]. Specifically, we identified a T1-weighted image as our study-specific template from a pool of 17 randomly selected subjects by examining deformations after morphing them to each other. Statistical analyses were performed using data registered to this template.

2.5. Statistical Methods

To determine if PI measured in different vessels carries different information, we computed full correlation matrix of PI in each vessel with PI in all other vessels.

Clusters of voxels with significant correlations of FA and PI were identified using voxel-wise *t*-test within a white matter mask and adjusted for age, gender and years of education.

The white matter mask was delineated over the template's T1-weighted image using FreeSurfer [29, 30]. We did not control for handedness because a prior study did not find significant differences between dominant and non-dominant hemispheres [16]. Correlations were considered significant at the voxel-level p-value threshold of $p < 0.005$. To control overall type-I error (false positive) rate to below 0.01 we only retained contiguous clusters of such voxels at least 100mm^3 in size. These criteria have been previously validated [31, 32].

2.6. Analysis Pipeline

We built analysis pipeline modules using Matlab (The MathWorks, Inc., Natick, MA) and bash scripts having unified interfaces: first argument is the output file name and all other arguments to a script are its inputs. All images were stored in the compressed single-file NIFTI format; b-values, b-vectors, hypothesis, etc — in plain text. To store (anonymized) demographic data about the subjects and to manage images and analysis we used SQLite — an SQL relational database management system [33]. The pipeline modules were assembled into the processing pipeline using GNU Make (version 3.81, http://www.gnu.org/software/make/).

3. Results

The sample cohort consisted of 107 subjects (55.2% female) with a mean age of 78 years (standard deviation 5, range 70 – 91) and mean number of years of education 14.5 (standard deviation 3.5). The mean values for systolic and diastolic blood pressure were 128 and 78 mmHg (standard deviations 10 and 7.1 respectively). PI in each examined artery are summarized in Fig. 1. Mean values of PI vary across arteries and generally increase in more distal arterial segments.

Correlation coefficients between all pairs of PIs are presented in Table 1. Overall, the correlations are modest with the highest correlation coefficient of 0.66 detected between the left and the right PCAs suggesting that PIs from different arteries do not provide identical information. Table 1 shows that PI in the right PCA exhibits highest correlations with that in the other vessels while PI in the BA — the lowest.

The pulsatility indices were not found to correlate with age as summarized in Table 2. This is consistent with the earlier work showing only a weak correlation of PI with age in a larger sample of EAS participants [34].

Clusters of voxels where FA is significantly correlated with age are shown in Fig. 2. A total of 23 clusters are detected, 19 exhibiting negative correlation (older age is associated with lower FA) and 4 positive. The total volumes of these sets are 11665mm^3 and 1520mm^3 respectively.

The summary of clusters with significant correlations between PI and FA is given in Table 3. Both positive and negative correlations are observed with negative correlations (higher PI is associated with lower FA) prevailing. Clusters with positive correlations did not intersected with clusters where FA is associated with age. Overlap of clusters with negative correlations and those in the age analysis is summarized in the last column of Table 3.

4. Discussion

In this study we demonstrated that pulsatility index in the cerebral arteries is correlated with FA, an early marker of WM integrity [14]. Further, the relation of PI to FA depends on artery and brain region. Because correlations among pulsatility indexes measured in each of the main cerebral arteries were modest (Table 1), analytic approaches that average their values across vessels to reduce noise, improve precision and/or to reduce the number of variables may dilute associations of PI and FA. Moreover, averaging may be performed in different ways yielding different effects on information: *(i)* average velocity time series across the vessels before extracting global PSV, EDV and MFV followed by applying the Gosling equation, *(ii)* average PSV, EDV and MFV extracted from each vessel prior to applying the Gosling equation and *(iii)* average PIs from each vessel [7, 12, 13, 35].

Prior studies have reported inconsistent results for the association between PI and white matter measures (FA and/or WMHI) [7, 12, 13, 35]. Our results suggest that this may be due to the fact that PIs in different vessels carry different information and that prior studies employed different methods of PI and spatial averaging. Other methodological differences, such as choice of b-value for DTI acquisition, may also be important. We used b-value=800sec/mm^2 because prior studies demonstrated this to be close to the optimal diffusion weighting for precise diffusion estimation [36, 37].

Unlike previous work, we considered PI from each artery independently and used a voxel-wise approach to determine which areas of white matter exhibit significant associations between PI and FA (Table 3, Figure 3). Analyses of PIs in the right VA and left MCA yield the largest number of clusters with the largest total volume where elevated PI is associated with lower FA. We pay particular attention to these negative correlations because at least one component mechanism of white matter degeneration, demyelination, manifests as lower than normal FA [38] and is associated with both aging and cognitive decline [39]. We, therefore, also determined areas where age-related decline in FA is significant (Figure 2) and found that overlap of these areas with those related to PIs is small, less than 13.3% (last column in Table 3). The largest overlap is with areas related to PI in left PCA. We conclude that areas of microstructural changes in WM related to elevated PI can not be explained by the age-related changes identified in prior research [39–41], because age was one of the covariates in PI - FA analysis and because overlap between areas where FA is associated with both PI and age is small. Conversely, prior studies reporting age-related changes in FA without regard to PI remain valid because PI appears to be an independent factor. And finally, PI is not likely a mediator of relationship of age to FA in this age group because of the very low correlation between age and PI (Table 2).

White matter areas where low FA is associated with elevated PI are not found to be limited to the vascular territory of the vessel where PI is assessed. For example, elevated PI in the left MCA is associated with lower FA regions within both the left and right hemispheres in Figure 3. This suggests that linkage between elevated PI and reduced FA is not through a direct downstream perfusion deficit within the territory of the affected artery. It is difficult, however, to establish the exact mechanism linking PI to white matter changes because interpretation of PI is confounded by the sensitivity of the index to blood pressure, pulse

rate, interplay of stiffness of vessels distal and proximal to the measurement site, microvascular resistance, blood viscosity, and in the case of cerebral circulation to intracranial pressure [16, 42]. Nevertheless, our observations are consistent with the hypothesis that microstructural changes are caused by increased mechanical waves emanating from pulsating vessel walls and traveling without much attenuation within the brain [43]. In this scenario we do not expect PI in an individual artery to be related to microstructural changes in regions specific to the arterial vascular territory. At the same time, we observe some spatial relation because elevated PI in different arteries is associated with reduced FA in essentially disjoint regions. Shear waves with their few centimeter wavelengths in the white matter at low frequencies could be the mechanistic basis for pulsatility-related white matter damage [44].

A potential limitation of this study and its conclusions is the fact that not all study subjects were eligible for or volunteered for MRI, potentially resulting in selection bias. However, care was taken to include subjects representative of the full Einstein Aging Study cohort. Indeed, at the time of the EAS enrollment, the sample of subjects who subsequently underwent MRI and TCD was slightly younger (75.1 versus 77.0 years), had a lower proportion of women (55.1% versus 66.8%) but similar years of education and race/ethnicity characteristics compared to the full EAS cohort [17].

5. Conclusion

In normal elderly subjects, elevated PI is related to lower FA, a marker of degraded white matter integrity. Areas of reduced FA are not limited to the vascular territory of the artery where PI is assessed and are distinct from areas with age-related FA changes. This suggests that elevated PI is a potential marker of low FA, independent of aging, but not necessarily as an indication of diminished perfusion. Instead, we support earlier implications of pulse wave injury to white matter [12, 43], which can be detected using low cost, portable and noninvasive TCD.

Acknowledgments

This work was supported by the National Institutes of Health [grant numbers AG03949, NINDS K24 NS 062737].

References

1. Prins ND, van Dijk EJ, den Heijer T, Vermeer SE, Jolles J, Koudstaal PJ, Hofman A, Breteler MMB. Cerebral Small-Vessel Disease and Decline in Information Processing Speed, Executive Function and Memory. Brain. 2005; 128:2034. [PubMed: 15947059]
2. Llewellyn DJ, Lang IA, Xie J, Huppert FA, Melzer D, Langa KM. Framingham Stroke Risk Profile and Poor Cognitive Function: A Population-Based Study. BMC Neurology. 2008; 8:12. [PubMed: 18430227]
3. Bangen KJ, Delano-Wood L, Wierenga CE, McCauley A, Jeste DV, Salmon DP, Bondi MW. Associations Between Stroke Risk and Cognition in Normal Aging and Alzheimer's Disease with and without Depression. Int J Geriatr Psychiatry. 2010; 25:175. [PubMed: 19551707]
4. Pantoni L. Cerebral Small Vessel Disease: From Pathogenesis and Clinical Characteristics to Therapeutic Challenges. Lancet Neurol. 2010; 9:689. [PubMed: 20610345]

5. Allan CL, Sexton CE, Kalu UG, Mcdermott LM, Kivimäki M, Singh-Manoux A, Mackay CE, Ebmeier KP. Does the Framingham Stroke Risk Profile Predict White-Matter Changes in Late-Life Depression? Int Psychogeriatrics. 2012; 4:524.
6. Wardlaw JM, Smith C, Dichgans M. Mechanisms of Sporadic Cerebral Small Vessel Disease: Insights from Neuroimaging. Lancet Neurol. 2013; 12:483. [PubMed: 23602162]
7. Kidwell CS, El-Saden S, Livshits Z, Martin NA, Glenn TC, Saver JL. Transcranial Doppler Pulsatility Indices as a Measure of Diffuse Small-Vessel Disease. J Neuroimaging. 2001; 11:229. [PubMed: 11462287]
8. Bateman GA. Pulse-Wave Encephalopathy: A Comparative Study of the Hydrodynamics of Leukoaraiosis and Normal Pressure Hydrocephalus. Neuroradiology. 2002; 44:740. [PubMed: 12221445]
9. Bateman GA, Levi CR, Schofield P, Wang Y, Lovett EC. The Venous Manifestations of Pulse Wave Encephalopathy: Windkessel Dysfunction in Normal Aging and Senile Dementia. Neuroradiology. 2008; 50:491. [PubMed: 18379767]
10. Mitchell GF, van Buchem MA, Sigurdsson S, Gotal JD, Jonsdottir MK, Kjartansson Ó, Garcia M, Aspelund T, Harris TB, Gudnason V, Launer LJ. Arterial Stiffness, Pressure and Flow Pulsatility and Brain Structure and Function: the Age, Gene/Environment Susceptibility — Reykjavik Study. Brain. 2011; 134:3398. [PubMed: 22075523]
11. Mok V, Ding D, Fu J, Xiong Y, Chu WWC, Wang D, Abrigo JM, Yang J, Wong A, Zhao Q, Guo Q, Hong Z, Wong KS. Transcranial Doppler Ultrasound for Screening Cerebral Small Vessel Disease: A Community Study. Stroke. 2012; 43:2791. [PubMed: 22949475]
12. Jolly TAD, Bateman GA, Levi CR, Parsons MW, Michie PT, Karayanidis F. Early Detection of Microstructural White Matter Changes Associated with Arterial Pulsatility. Front Hum Neurosci. 2013; 7:782. [PubMed: 24302906]
13. Purkayastha S, Fadar O, Mehregan A, Salat DH, Moscufo N, Meier DS, Guttmann CRG, Fisher NDL, Lipsitz LA, Sorond FA. Transcranial Doppler Velocities in a Large, Healthy Population. J Cereb Blood Flow Metabol. 2014; 34:228.
14. Chua TC, Wen W, Slavin MJ, Sachdev PS. Diffusion Tensor Imaging in Mild Cognitive Impairment and Alzheimer Disease: A Review. Currrent Opinion in Neurology. 2008; 21:83.
15. Gosling RG, King DH. Arterial Assessment by Doppler Shift Ultrasound. Proc R Soc Med. 1974; 67:447. [PubMed: 4850636]
16. Tegeler CH, Crutchfield K, Katsnelson M, Kim J, Tang R, Passmore Griffin L, Rundek T, Evans G. Transcranial Doppler Velocities in a Large, Healthy Population. J Neuroimaging. 2013; 23:446.
17. Katz MJ, Lipton RB, Hall CB, Zimmerman ME, Sanders AE, Verghese J, Dickson DW, Derby CA. Age-Specific and Sex-Specific Prevalence and Incidence of Mild Cognitive Impairment, Dementia, and Alzheimer Dementia in Blacks and Whites: A Report from the Einstein Aging Study. Alzheimer Dis Assoc Disord. 2012; 26:335. [PubMed: 22156756]
18. Alexandrov AV, Sloan MA, Wong LK, Douville C, Razumovsky AY, Koroshetz WJ, Kaps M, Tegeler CH. Practice Standards for Transcranial Doppler Ultrasound: Part I — Test Performance. J Neuroimaging. 2007; 17:11. [PubMed: 17238867]
19. Smith SM, Jenkinson M, Woolrich MW, Beckmann CF, Behrens TEJ, Johansen-Berg H, Bannister PR, De Luca M, Drobnjak I, Flitney DE, Niazy RK, Saunders J, Vickers J, Zhang Y, De Stefano N, Brady JM, Matthews PM. Advances in Functional and Structural MR Image Analysis and Implementation as FSL. NeuroImage. 2004; 23(Suppl 1):S208. [PubMed: 15501092]
20. Jenkinson M, Beckmann CF, Behrens TEJ, Woolrich MW, Smith SM. FSL, NeuroImage. 2012; 62:782. [PubMed: 21979382]
21. Smith SM, Johansen-Berg H, Jenkinson M, Rueckert D, Nichols TE, Miller KL, Robson MD, Jones DK, Klein JC, Bartsch AJ, Behrens TEJ. Acquisition and Voxelwise Analysis of Multi-Subject Diffusion Data with Tract-Based Spatial Statistics. Nature Protocols. 2007; 2:499. [PubMed: 17406613]
22. Jezzard P, Balaban RS. Correction for Geometric Distortion in Echo-Planar Images from B_0 Fiend Variations. Magn Reson Med. 1995; 34:65. [PubMed: 7674900]
23. Cusack R, Brett M, Osswald K. An Evaluation of the Use of Magnetic Field Maps to Undistort Echo-Planar Images. NeuroImage. 2003; 18:127. [PubMed: 12507450]

24. Good CD, Johnsrude IS, Ashburner J, Henson RNA, Friston KJ, Frackowiak RSJ. A Voxel-Based Morphometric Study of Ageing in 465 Normal Adult Human Brains. NeuroImage. 2001; 14:21. [PubMed: 11525331]
25. Ardekani BA, Braun M, Hutton BF, Kanno I, Iida H. A Fully Automatic Multimodality Image Registration Algorithm. NeuroImage. 1995; 19:615.
26. Ardekani BA, Guckemus S, Bachman A, Hoptman MJ, Wojtaszek M, Nierenberg J. Quantitative Comparison of Algorithms for Inter-Subject Registration of 3D Volumetric Brain MRI Scans. J Neurosci Methods. 2005; 142:67. [PubMed: 15652618]
27. Klein A, Andersson J, Ardekani BA, Ashburner J, Avants B, Chiang MC, Christensen GE, Collins DL, Gee J, Hellier P, Song JH, Jenkinson M, Lepage C, Rueckert D, Thompson P, Vercauteren T, Woods RP, Mann JJ, Parsey RV. Evaluation of 14 Nonlinear Deformation Algorithms Applied to Human Brain MRI Registration. NeuroImage. 2009; 46:786. [PubMed: 19195496]
28. Smith SM, Jenkinson M, Johansen-Berg H, Rueckert D, Nichols TE, Mackay CE, Watkins KE, Ciccarelli O, Cader MZ, Matthews PM, Behrens TEJ. Tract-Based Spatial Statistics: Voxelwise Analysis of Multi-Subject Diffusion Data. NeuroImage. 2006; 31:1487. [PubMed: 16624579]
29. Fischl B, Salat DH, Busa E, Albert M, Dieterich M, Haselgrove C, van der Kouwe A, Killiany R, Kennedy D, Klaveness S, Montillo A, Makris N, Rosen B, Dale AM. Whole Brain Segmentation: Automated Labeling of Neuroanatomical Structures in the Human Brain. Neuron. 2002; 33:341. [PubMed: 11832223]
30. Fischl B, Salat DH, van der Kouwe AJ, Makris N, Segonne F, Quinn BT, Dale AM. Sequence-Independent Segmentation of Magnetic Resonance Images. NeuroImage. 2004; 23(Suppl 1):S69. [PubMed: 15501102]
31. Lipton ML, Gellella E, Lo C, Gold T, Ardekani BA, Shifteh K, Bello JA, Branch CA. Multifocal White Matter Ultrastructural Abnormalities in Mild Traumatic Brain Injury with Cognitive Disability: A Voxel-Wise Analysis of Diffusion Tensor Imaging. J Neurotrauma. 2008; 25:1335. [PubMed: 19061376]
32. Suri AK, Fleysher R, Lipton ML. Subject Based Registration for Individualized Analysis of Diffusion Tensor MRI. PLoS One. 2015; 10:e0142288. [PubMed: 26580077]
33. Hipp, DR., Kennedy, D., Mistachkin, J. SQLite. (Version 3.8.8.3), https://www.sqlite.org/, retrieved on February 25, 2015
34. Yang D, Cabral D, Gaspard EN, Lipton RB, Rundek T, Derby CA. Cerebral Hemodynamics in Elderly: A Transcranial Doppler Study in the Einstein Aging Study (EAS) Cohort. J Ultrasound in Medicine. in press.
35. Del Brutto OH, Mera RM, de la Luz Andrade M, Castillo PR, Zambrano M, Nader JA. Disappointing Reliability of Pulsatility Indices to Identify Candidates for Magnetic Resonance Imaging Screening in Population-Based Studies Assessing Prevalence of Cerebral Small Vessel Disease. J Neurosciences Rural Practice. 2015; 6:336.
36. Xing D, Papadakis N, Huang C, Lee V, Carpenter T, Hall L. Optimized Diffusion-Weighting for Measurement of Apparent Diffusion Coefficient (ADC) in Human Brain. Magn Reson Imag. 1997; 15:771–784.
37. Fleysher R, Fleysher L, Gonen O. The Optimal MR Acquisition Strategy for Exponential Decay Constants Estimation. Magn Reson Imag. 2008; 26:433.
38. Song SK, Sun SW, Ramsbottom MJ, Chang C, Russell J, Cross AH. Dysmyelination Revealed Through MRI as Increased Radial (but Unchanged Axial) Diffusion of Water. NeuroImage. 2002; 17:1429. [PubMed: 12414282]
39. Grieve SM, Williams LM, Paul RH, Clark CR, Gordon E. Cognitive Aging, Executive Function, and Fractional Anisotropy: A Diffusion Tensor MR Imaging Study. AJNR. 2007; 28:226. [PubMed: 17296985]
40. Pfefferbaum A, Sullivan E, Hedehus M, Lim K, Adalsteinsson E, Moseley M. Age-Related Decline in Brain White Matter Anisotropy Measured with Spatially Corrected Echo-Planar Diffusion Tensor Imaging. Magn Reson Med. 2000; 44:259. [PubMed: 10918325]
41. Kochunov P, Williamson DE, Lancaster J, Fox P, Cornell J, Blangero J, Glahn DC. Fractional Anisotropy of Water Diffusion in Cerebral White Matter Across the Lifespan. Neurobiology of Aging. 2012; 33:9. [PubMed: 20122755]

42. Michel E, Zernikow B. Goslings Doppler Pulsatility Index Revisited. Ultrasound Med Biol. 1998; 24:597. [PubMed: 9651969]

43. Bateman GA. Pulse Wave Encephalopathy: A Spectrum Hypothesis Incorporating Alzheimer's Disease, Vascular Dementia and Normal Pressure Hydrocephalus. Med Hypotheses. 2004; 62:182. [PubMed: 14962623]

44. Kruse SA, Rose GH, Glaser KJ, Manduca A, Felmlee JP, Jack CR Jr, Ehman RL. Magnetic Resonance Elastography of the Brain. NeuroImage. 2008; 39:231. [PubMed: 17913514]

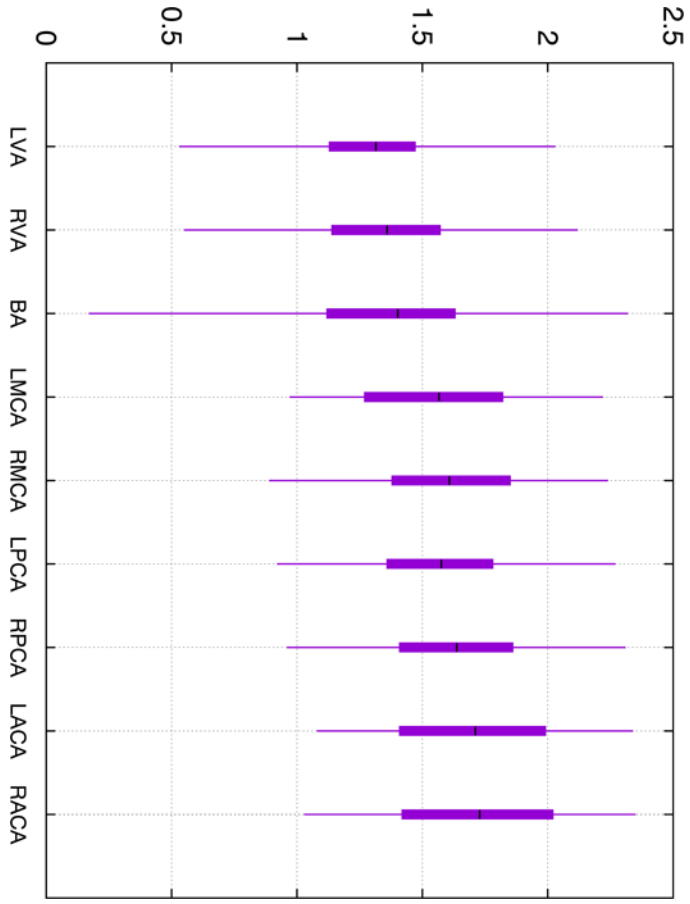

Figure 1.

Candlestick plot of the pulsatility index in all examined cerebral arteries. Whiskers indicate minimum and maximum value in the sample, bars — 25 and 75 percentiles and horizontal mark — mean value. Prefixes “L” and “R” indicate left and right respectively.

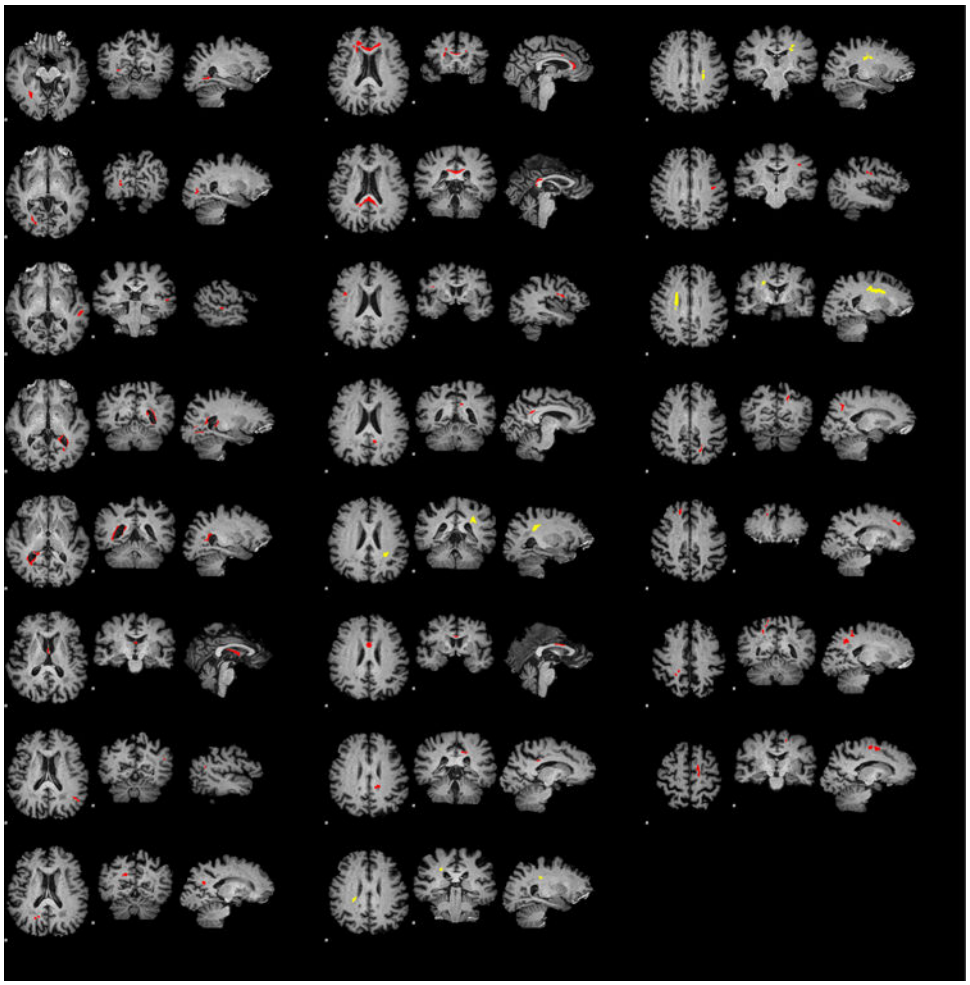

Figure 2.

Clusters of voxels with significant correlations of FA and age. Clusters with negative correlations where older age is associated with lower FA are marked in red. Those with positive correlations — in yellow.

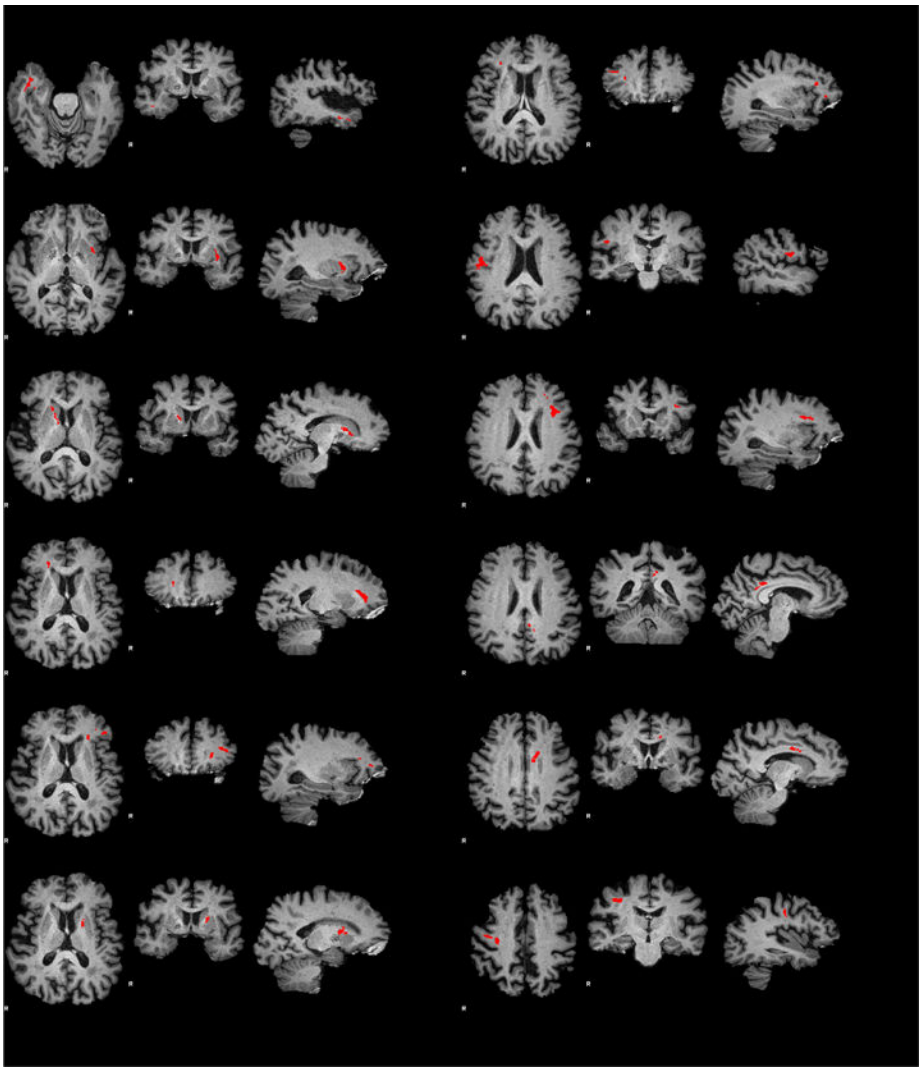

Figure 3.

Clusters of voxels (red) with significant correlations of FA and pulsatility index in left MCA. All correlations were negative: higher pulsatility is associated with lower FA. See Table 3 for summary of clusters in all examined arteries.

Table 1

Table of Pearson correlation coefficients between pulsatilities in all examined arteries.

	left VA	right VA	BA	left MCA	right MCA	left PCA	right PCA	left ACA	right ACA
left VA	1.00	0.50	0.21	0.30	0.27	0.33	0.30	0.25	0.34
right VA	0.50	1.00	0.11	0.32	0.28	0.33	0.18	0.13	0.10
BA	0.21	0.11	1.00	0.12	0.20	0.28	0.32	−0.05	0.35
left MCA	0.30	0.32	0.12	1.00	0.63	0.56	0.61	0.51	0.46
right MCA	0.27	0.27	0.20	0.63	1.00	0.60	0.61	0.41	0.55
left PCA	0.33	0.33	0.28	0.56	0.60	1.00	0.66	0.41	0.54
right PCA	0.30	0.18	0.32	0.61	0.61	0.66	1.00	0.55	0.64
left ACA	0.25	0.13	−0.05	0.51	0.41	0.41	0.55	1.00	0.62
right ACA	0.34	0.10	0.35	0.46	0.55	0.54	0.64	0.62	1.00

Magn Reson Imaging. Author manuscript; available in PMC 2019 April 01.

Table 2

Pearson correlation coefficients (ρ) and their statistical significance (number of standard deviations, σ) between age and pulsatility in the examined arteries. Note that number of subjects (N) where pulsatility data is available varied with vessel due to normal anatomical variations in “acoustic window” for TCD. No statistically significant relations are observed.

artery	ρ	σ	N
left VA	+0.002	0.024	104
right VA	+0.032	0.329	105
BA	−0.121	1.230	102
left MCA	+0.011	0.102	80
right MCA	+0.040	0.363	83
left PCA	−0.085	0.729	74
right PCA	+0.010	0.091	78
left ACA	+0.048	0.409	73
right ACA	−0.101	0.892	78

Table 3

Number of FA clusters and their total volume with positive (“+”) and negative (“−”) correlations between FA and pulsatility index in each examined artery. Number of subjects is the same as in Table 2. Last column is volume of intersection of clusters with negative correlations and clusters in aging analysis presented in Figure 2. Clusters with positive correlations had no such overlap.

artery	+Count	−Count	+Volume (mm^3)	−Volume (mm^3)	−Intersection (mm^3)
left VA	1	5	127	852	96
right VA	0	13	0	3031	228
BA	0	0	0	0	0
left MCA	0	12	0	3210	181
right MCA	0	3	0	421	0
left PCA	0	11	0	1994	266
right PCA	1	7	152	981	6
left ACA	2	1	248	319	3
right ACA	0	11	0	1635	193